IEEE Access
Multidisciplinary | Rapid Review | Open Access Journal

Received November 4, 2020, accepted November 11, 2020, date of publication November 17, 2020,
date of current version December 2, 2020.

Digital Object Identifier 10.1109/ACCESS.2020.3038428

Peripheral Dimming: A New Low-Power Technology for OLED Display Based on Gaze Tracking

JEONG-SIK KIM AND SEUNG-WOO LEE, (Senior Member, IEEE)
Department of Information Display, Kyung Hee University, Seoul 02447, South Korea

Corresponding author: Seung-Woo Lee (seungwoolee@khu.ac.kr)

This work was supported in part by the BK21 FOUR (Fostering Outstanding Universities for Research) funded by the Ministry of Education (MOE, South Korea), and in part by the National Research Foundation of Korea (NRF) grant funded by the Korea Government (MSIT) under Grant 2020R1F1A1076479.

ABSTRACT In this paper, a new low-power technology based on gaze tracking, called peripheral dimming, is proposed for organic light-emitting diode (OLED) displays. The goal of the proposed method is to save power without degrading the perceptual image quality. In the proposed method, the peripheral vision area on the screen is gradually darkened depending on the distance from the gaze point. In this work, quantitative conditions for preventing degradation of the perceived image quality are studied through a psychophysical experiment by using three video clips. We suggest a lightness reduction ratio (LRR) that determines the amount of reduced luminance per viewing angle based on the lightness. Four conditions of the LRR from 0.1 to 1.0%/degree are applied to each clip. The experiment is designed based on a two-alternative forced choice: a test clip with the proposed method is compared to the original one, and subjects are forced to choose the brighter clip between the two clips shown in random order. In this way, the threshold of the LRR from which people begin to notice a difference between the test and original clips is obtained. The experimental results demonstrate that the proposed method saves the power of OLED displays up to 34.4% while keeping the image quality high in terms of both subjective and objective quality (the mean structural similarity index is higher than 0.94). Therefore, the proposed method will help to enable low-power operation of OLED displays used for head-mounted display devices while maintaining the quality of experience.

INDEX TERMS Low-power technology, organic light emitting diode (OLED) display, gaze tracking, human visual system (HVS), quality of experience (QoE), peripheral vision.

I. INTRODUCTION

An organic light-emitting diode (OLED) display is a representative self-luminous display. It has many advantages over liquid crystal displays (LCDs) in terms of viewing angle, color gamut, response speed, thickness, and so on [1]–[3]. For this reason, OLED displays are rapidly becoming the mainstream displays for mobile devices such as smartphones and head-mounted displays (HMDs).

Displays have been developed to achieve superior image quality with higher resolution and higher luminance. The luminance of an OLED is determined by the electric current flowing through it [4]. This means that power consumption could be reduced by limiting the luminance. By using this characteristic, hardware-based [5]–[7] and software-based [8]–[17] low-power techniques have been studied. Shin *et al.* [5] proposed a dynamic voltage scaling technique that dynamically changes the supply voltage of an OLED panel to limit the maximum luminance. Oh *et al.* presented a light-and-space-adaptable (LASA) display that can switch between emissive and reflective display modes depending on ambient light [6]. By turning off all OLED pixels and running the reflective display mode in a bright environment, the LASA display can realize a brighter screen and lower power consumption. A net power control (NPC) that modifies pixel data when the total current is larger than a threshold value was proposed to save power [7]. Although these techniques can save electric power efficiently, their application to real devices is limited because they need their own specific hardwares such as a newly

The associate editor coordinating the review of this manuscript and approving it for publication was Muhammad Zubair.

designed pixel circuit or a new display device for mode switching.

Generally, there is a trade-off between the saved power and image quality, which is a part of the quality of experience (QoE). Some research groups have attempted to optimize the power-saving condition based on the objective image quality assessment (IQA) [8]–[12]. Brightness scaling (BS), which modifies brightness by remapping the gray-level curve, is a typical power-saving solution [8]–[10]. Although the contrast ratio of the image would be reduced in these techniques owing to the decrease in the peak luminance, they minimize image quality degradation by determining the most efficient condition based on the objective IQA. Contrast enhancement (CE) is a technique to achieve image CE as well as power saving. Lee *et al.* presented a histogram-based power-constrained CE algorithm (PCCE) for emissive displays, which can enhance image contrast and reduce power consumption [11]. Pagliari *et al.* presented low-overhead adaptive power saving and contrast enhancement, called LAPSE [12], where the overhead was improved from [11]. From the BS to CE techniques, their approaches seem to achieve the most efficient trade-off between power saving and image quality based on the objective IQA. However, this type of technique has a problem in that objective IQAs do not perfectly reflect the actual perceived image quality, that is, a human might perceive significant differences in image quality.

Some researchers have studied human visual system (HVS)-based approaches [13]–[17]. Park *et al.* [13] reduced the brightness of video via alpha blending. They examined the acceptability of brightness degradation through a user study. However, this study has a limitation owing to computing overhead in mobile devices. Choubey *et al.* have attempted to turn off selective subpixels to display a graphic user interface (GUI) with a lower resolution but higher than human visual acuity [14]. They suggested an optimum subpixel arrangement that could minimize color degradation with efficient power. A number of studies have focused on visually perceived information with a user study. For example, the edge of the screen when playing first-person shooting (FPS) games [15], [16] or the screen area covered by users' fingers when using a mobile phone [17] is not the users' main focus of attention. These approaches achieved power saving without incurring significant usability impact by performing a user study. However, these techniques have a problem in that the area of the focus of attention does not always correspond to the area where the user actually sees. For example, when playing FPS games, the user mainly sees a crosshair at the center of the screen but not always. In this case, the dimming region could be a hindrance to the game. To overcome the application limitation, we decided to investigate a technique that can interact with users.

This paper proposes a new low-power technology based on gaze tracking, called peripheral dimming. It reduces the luminance of the pixels in the peripheral vision on an OLED display screen. This study is motivated by the foveated rendering technology, which reduces the rendering workload in the peripheral vision by using an eye tracker [18]. Herein, we suggest an HVS-based criterion for the proposed method, called a lightness reduction ratio (LRR). A psychophysical experiment and statistical analysis were performed to verify the proposed method. In addition, the LRR threshold, where power consumption becomes minimized without visual image degradation, is found from psychometric experiments.

This paper is organized as follows. Section II presents the theoretical background. In Section III, the proposed method and its objectives are introduced. In sections IV and V, the design of the psychophysical experiment and the experimental results are given, respectively. The conclusion is presented in Section VI.

II. BACKGROUND

A. POWER MODEL OF OLED DISPLAY

The power consumption in an OLED display depends on its luminance. Strictly speaking, the power consumed by a pixel of the OLED display is proportional to the linear RGB values [19]. The linear RGB values have a linear relationship with the luminance (gamma-expanded values). According to the previous study [20], the power consumption in a pixel of the OLED display panel can be modeled by

$$P_{display} = f(R) + f(G) + f(B) + C \tag{1}$$

where $f(\mathrm{R})$, $f(\mathrm{G})$, and $f(\mathrm{B})$ denote the power consumption of the red, green, and blue subpixels, respectively. C accounts for the static power consumed by non-pixel parts. Herein, the power consumption of each subpixel is expressed as follows:

$$f(X) = \omega_x X^{\Upsilon} \tag{2}$$

where X and ω_x are digital RGB data and weighting component, respectively. Exponent γ denotes the gamma value, which is typically 2.2. Because the weighting component is related to the physical characteristics of the OLED display panel, its value may vary depending on the OLED panel. In this study, the same coefficients adopted from [11] and [21], $(\omega_r{:}\omega_g{:}\omega_b) = (70{:}115{:}154)$, are used.

In this work, we ignore the static power consumed by non-pixel parts, C in (1), because only the pixel values are handled. As a result, the total dissipated power (TDP) for displaying a color image is given by [11]

$$TDP = \sum_{i=1}^{N}\sum_{j=1}^{M}\left\{f(R_{i,j}) + f(G_{i,j}) + f(B_{i,j})\right\} \tag{3}$$

where i and j denote the horizontal and vertical indices of a pixel, respectively, and N and M denote the numbers of the horizontal and vertical pixels, respectively. $R_{i,j}$, $G_{i,j}$, and $B_{i,j}$ denote the RGB levels of the pixel (i, j).

B. HUMAN VISUAL SYSTEM

The retina has a number of photoreceptor cells (rod and cone cells). The cone cells are responsible for color vision in bright light. The rod cells, on the other hand, are more

sensitive cells and respond to less intense light than the cone cells. Their distribution throughout the retina is not uniform, as shown in Fig. 1(a). The cone cells are densely packed in the fovea, and their number quickly decreases in the periphery of the retina, whereas the rod cells are usually concentrated in the periphery of the retina. The number of the rod cells gradually decreases from the peak position, as shown in Fig. 1(a) [22]. In a typical bright environment, the cone cells are dominant in the vision, which is called photopic vision [23], as shown in Fig. 1(b). As relatively few cone cells exist in the periphery of the retina, we anticipated that the peripheral vision would be insensitive to changes in brightness.

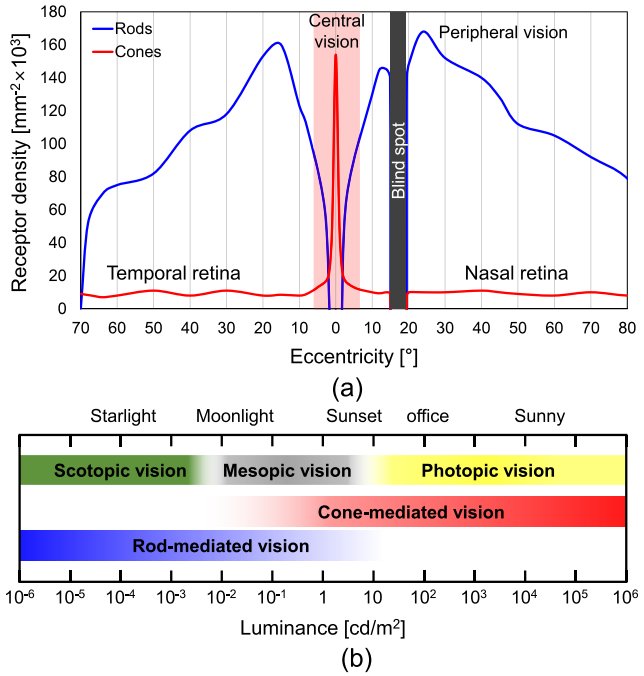

FIGURE 1. (a) Distribution of rods and cones depending on the eccentricity from the fovea of the human eye [22] and (b) approximate ranges of the photoreceptor regimes [23].

Human vision has a nonlinear relationship between perceived brightness and luminance. For example, the human eye is able to detect a luminance change sensitively when a dark image becomes darker or brighter, whereas it is insensitive to changes in luminance of a bright part. The CIELAB color space is intended to match the capabilities of the HVS. The lightness (L*) is intended to match a subjective perception of brightness among the components of the CIELAB color space. The L* is expressed as a power function of the luminance as follows:

$$L^* = 116f\left(\frac{Y}{Y_w}\right) - 16,$$
$$f(t) = \begin{cases} t^{1/3}, & \text{if } t > \left(\frac{6}{29}\right)^3 \\ \frac{1}{3}\left(\frac{29}{6}\right)^2 t + \frac{4}{29}, & \text{otherwise} \end{cases} \quad (4)$$

where Y and Y_w are the luminance of a pixel and white pixel, respectively. The L* is determined from 0 to 100, where 0 and 100 correspond to black and white, respectively.

C. PSYCHOPHYSICAL ANALYSIS

This work is based on psychophysics, which is the scientific study of the relationship between stimulus and sensation [24]. There are several techniques for measuring responses, of which the two-alternative forced choice (2-AFC) method is used in this study. A subject is forced to choose one of the two alternative options, and then the correct answer rate is obtained. When two stimuli are indistinguishable, they are chosen on a 50:50 ratio. Thus, the correct answer rate is from 50% to 100% in the 2-AFC method. We determined the stimulus intensity at a 75% correct response rate as the threshold level. The threshold is the point of intensity at which the subject can detect the presence of a difference between two stimuli [24]. Stimuli with intensities below the threshold are considered undetectable.

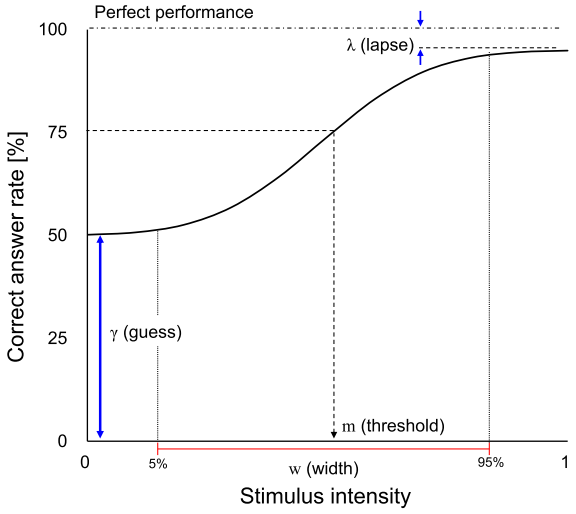

FIGURE 2. Example of the psychometric function and parameters.

The psychometric function is a useful analysis tool to estimate the threshold of the stimulus intensity statistically. It is an inferential model that describes the relationship between the underlying probability of the correct (or positive) responses and the stimulus intensity. This model typically curves an S-shaped function, the so-called sigmoid curve, as shown in Fig. 2. The psychometric function (ψ) is defined with a sigmoid function (S) and two upper and lower asymptotes, lapse (λ) and guess (γ), as follows [25]:

$$\psi(x; m, w, \lambda, \gamma) = \gamma + (1 - \lambda - \gamma)S(x; m, w)$$
$$S(x; m, w) = \frac{1}{\sqrt{2\pi}} \int_{-\infty}^{(x-m)/w} e^{-t^2/2} dt \quad (5)$$

where λ denotes the probability of the incorrect answer at infinitely high stimulus levels. The parameter γ, which denotes the correct answer for infinitely low stimulus levels, depends on the experimental condition. In the 2-AFC method,

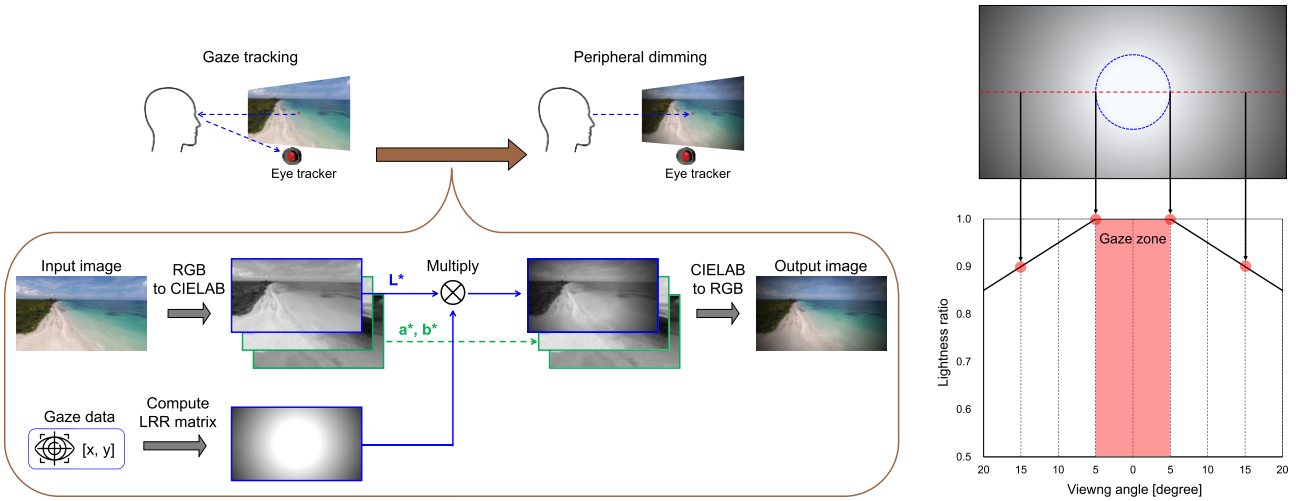

FIGURE 3. (a) Framework of the proposed method and (b) lightness ratio depending on the viewing angle in the case of gazing at the center of the screen.

it is 50%. The remaining parameters x, m, and w denote the stimulus level, threshold level, and width, respectively. The width is defined as the difference between the stimulus levels where the sigmoid function reaches 0.05 and 0.95. The sigmoid function used in this study was the cumulative Gaussian function, as described in (5). In this study, we used the psignifit 4 for MATLAB presented by Schütt *et al.* [25] to fit the psychometric function to our experimental data. This tool is an open-source package that estimates the psychometric function by fitting a beta-binomial model to the correct responses at each stimulus level based on Bayesian inference.

III. PROPOSED METHOD

A. PERIPHERAL DIMMING

We propose a peripheral dimming method based on gaze tracking that can save power efficiently without degradation of the perceptual image quality. The power consumption of the display is reduced by darkening the pixels in the peripheral vision area. Fig. 3(a) illustrates a framework of peripheral dimming when gazing at the center of the screen. In the proposed method, the input image is decomposed into the lightness (L*) and color components (a* and b*) via the color space conversion from RGB to CIELAB. Based on the gaze data, an LRR matrix is calculated and then multiplied to the L* image. The updated CIELAB is converted into the RGB color space, and the final image is displayed.

Fig. 3(b) shows the lightness ratio of the image depending on the viewing angle. The inner area enclosed by a blue dashed circle, invisible to people, with a viewing angle of 10° is defined as the gaze zone. The size of the gaze zone was determined with reference to the central vision area, as shown in Fig. 1(a). The pixels within the gaze zone maintain their original lightness. The pixels outside the gaze zone become gradually and linearly darker as they are farther from the gaze zone, as shown in Fig. 3(b). The reduction ratio of the lightness depending on the viewing angle is called the LRR, and its matrix is expressed as follows:

$$LRR_{px}(i,j) = \{VA_{px}(i,j) - VA_{gz}\} \times LRR_{cond} \tag{6}$$

where VA_{px} and VA_{gz} denote the viewing angles of the locations of (i, j) pixel from the gaze point and gaze zone, i.e., 10°, respectively. Indices (i, j) are the horizontal and vertical indices of a pixel, respectively. LRR_{cond} denotes the target LRR condition, which is the slope in Fig. 3(b). For example, if the viewing angle is 14° and the LRR_{cond} is 1%/°, the lightness of the pixel is reduced by 4%, (14°–10°) × 1%/°.

B. OBJECTIVE

The final objective of peripheral dimming is to reduce the power consumption of eye-tracker-integrated HMD devices such as virtual reality (VR)/augmented reality (AR) headsets. The proposed technique is simple; however, only a few studies have been conducted. For example, Wee *et al.* [16] presented a similar dimming method of darkening the edge of a display by using dimming boxes. They implemented the method on a mobile game and verified that it did not significantly affect playability. However, the numerical conditions for applying the method have not yet been presented. For example, the acceptable degree of the image brightness reduction of the peripheral vision area without degrading the image quality remains to be determined. We attempt to find an answer in this study. For this, it is necessary to determine the threshold LRR levels where the image brightness could be maximally reduced while maintaining the image quality. In addition, our method aims to develop a gaze-adaptive technique using an eye tracker, capable of actively reacting to the gaze at which the user is looking. Hence, it should be verified that the threshold levels can be applied to various types of gaze positions and even images. In this work, we focus on the effect of images; the gaze point is fixed to the center of the screen as the first step.

IV. PSYCOPHYSICAL EXPERIMENT

A. DESIGN

The experiment was designed based on two methods: double stimulus (DS) and 2-AFC [26], [27].

The former is one of the international recommendations for subjective video quality assessment, ITU-R BT.500-11 [26]. As shown in Fig. 4, an assessment unit of the DS method consists of a pair of videos. First, a fixation image that indicates the gaze position with the red crosshair is displayed for three seconds. Thereafter, reference and test (dimmed) videos are sequentially displayed for eight seconds in random order. A full-screen gray image is inserted between two videos for three seconds for a fair comparison. After the second stimulus, the subjects were given ten seconds to vote for the brighter video. The latter is a psychophysical method used to investigate behavioral or perceptual responses from subjects [27]. Subjects are forced to choose between two alternative stimuli. In this work, the subject was asked to choose the brighter video between the two videos during the voting sequence.

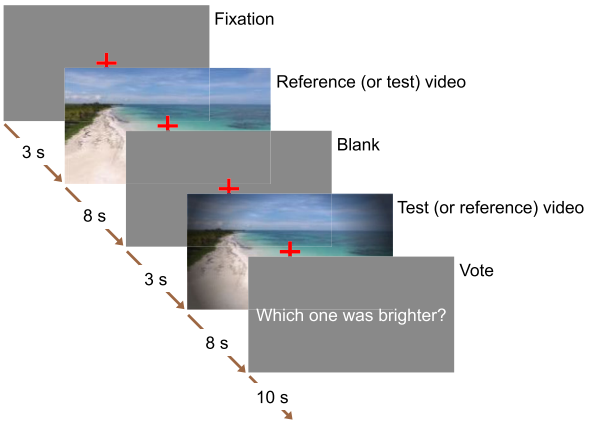

FIGURE 4. Schematic diagram of an assessment unit.

B. CONDITIONS

Three video clips with a 1920 × 1080 resolution were used. They were released under the Creative Commons CC0 [28]. Fig. 5 shows a frame image and the average lightness of each clip. We created test video clips with all frame images modified. Fig. 6 shows an example of the modified frame image. A red cross with a size of a 1° viewing angle is added to the center of the frame image as a gaze point. In addition, we set a virtual region, called allowed zone, with an 8° viewing angle to check the validity of the subject's answer. When the subject looked outside the allowed zone, a beep sounded as an alert. If the beep sounded more than three times within one assessment unit, the data were excluded from the data analysis.

In the experiment, four conditions of the LRR were used: 0.1, 0.4, 0.7, and 1.0%/degree. First, the color space was converted from RGB to CIELAB for all pixels. Thereafter, the lightness of pixels out of the gaze zone was modified based on the value of LRR_{px}. Finally, the color space was converted from CIELAB to RGB in reverse order to renew the pixel data. The test video clips depending on the LRR condition were made in advance.

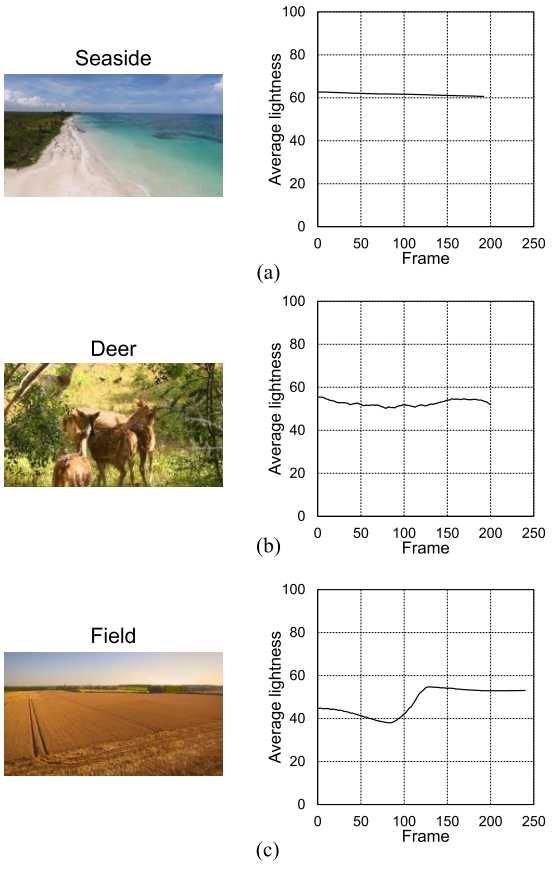

FIGURE 5. Frame image and average lightness of all frame images of (a) Seaside, (b) Deer, and (c) Field clips.

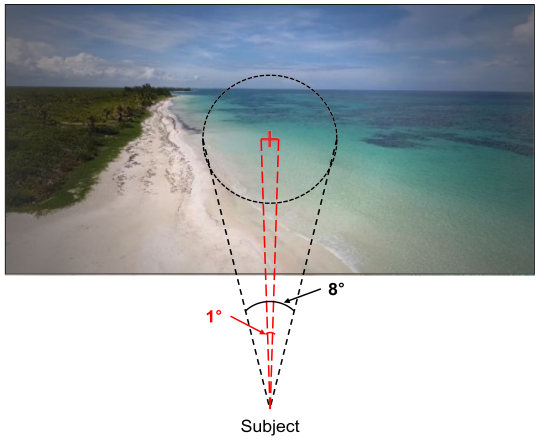

FIGURE 6. Added red cross with a 1° viewing angle and allowed zone with an 8° viewing angle in the frame image.

C. PROCEDURE

The experiment was conducted in a dark room. As shown in Fig. 7, a 24-inch LCD monitor with a 1920 × 1080 resolution was used, and it was 70 cm away from the subject. All subjects fixed their head in a chin rest. An eye tracker, Tobii eyeX, was used to obtain the gaze data.

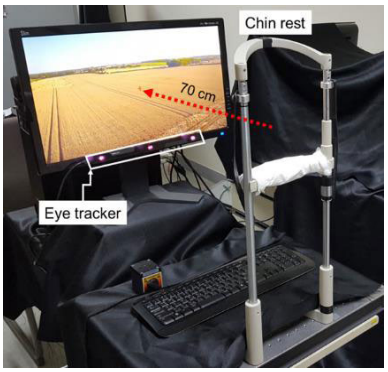

FIGURE 7. Experimental setup composed of an eye tracker, a monitor, and a chin rest.

Eight, twelve, and ten subjects participated in the experiment using Seaside, Deer, and Field video clips, respectively. Each subject watched only one type of video clip, and a total of thirty people participated in the experiment. Their average age was 23.3 years. After calibrating the eye tracker, the assessment unit started. After each assessment unit, the subjects were given ten seconds to choose the brighter video. We obtained an answer six times for each LRR condition, and consequently, the assessment unit was repeated 24 times for each video clip. It took about 15 min.

V. RESULTS

A. EXPERIMENTAL RESULTS

Table 1 shows the number of effective responses for each LRR condition of the three video clips.

TABLE 1. Number of effective responses under each condition.

LRR [%/degree]	# of effective responses (total count)		
	Seaside	Deer	Field
0.1	47 (48)	68 (72)	58 (60)
0.4	47 (48)	69 (72)	60 (60)
0.7	48 (48)	71 (72)	58 (60)
1.0	48 (48)	71 (72)	56 (60)

Fig. 8 shows the average correct answer rate per the LRR of the video clips. In the graph, black dots and error bars denote the average correct answer rate and the standard error, respectively. The detailed values are described in Table 2. The correct answer rates of all clips were close to 50%, where the LRR was set to 0.1%/degree. This means that the subjects could not notice any difference from the original clip under the condition. The correct answer rate progressively rises with the LRR level. In order to analyze the results statistically, a one-way analysis of variance (ANOVA) was performed. In the Seaside clip, the correct answer rates for LRR values of 0.1%/degree and 0.4%/degree were 44% and 92%, respectively, and they were significantly different ($p < 0.01$). Similarly, other clips also had at least one LRR condition where the correct answer rate was over 75%. The correct answer rate over 75% was significantly different from that at an LRR of 0.1%/degree for each video clip,

TABLE 2. Average correct answer rates per the LRR condition in each clip.

Video clip	Lightness reduction ratio [%/degree]			
	0.1	0.4	0.7	1.0
Seaside [%]	44	92	94	98
Deer [%]	45	69	79	88
Field [%]	51	57	68	78

as shown in Fig. 8. These results show that the threshold condition exists within the given LRR range, and the objective of the proposed method is realizable.

As mentioned in Section II, we assumed that the LRR value when the correct answer rate is equal to 75% is the threshold level (LRR_{TH}). To calculate LRR_{TH}, the psychometric function for the results was used, as shown in Fig. 9. In the graph, the blue dots and the black solid curve line denote the average correct answer rate and the estimated psychometric function, respectively. The obtained LRR_{TH} values were 0.29, 0.63, and 0.88%/degree for each clip of Seaside, Deer, and Field, respectively, as described in Table 3.

TABLE 3. Threshold levels of the LRR for each clip.

	Seaside	Deer	Field
LRR_{TH} [%/degree]	0.29	0.63	0.88

The results show that LRR_{TH} varies with the video clips. Thus, we compared LRR_{TH} for different average lightness values of the video clips, as shown in Fig. 10. In the graph, the open circle and the error bar denote the average and standard deviation of the lightness of all frame images. We anticipated that LRR_{TH} would be independent of the video clips because the amount of the reduced luminance was determined based on the lightness related to human brightness perception. However, the results show that LRR_{TH} is inversely proportional to the average lightness of the video clip. It seems that there is a strong relationship between LRR_{TH} and the lightness of an image. Although the data are not sufficient for a conclusion, it is possible that a quantitative model of LRR_{TH} would be determined in further studies.

The saved power amount based on the TDP described in (3) is computed as follows:

$$P_{SAVED} = (1 - \frac{TDP_{TH}}{TDP_{ORG}}) \times 100 \quad (7)$$

where TDP_{ORG} and TDP_{TH} denote the TDPs of the original video and that adopting LRR_{TH}, respectively. We obtained P_{SAVED} for all frame images and averaged them for each clip. Table 4 describes the TDP_{ORG}, TDP_{TH}, and P_{SAVED} values for each video clip.

The peripheral dimming method saves power consumption by an average of 11.0, 21.0, and 34.4% for the three video clips: Seaside, Deer, and Field, respectively, when the LRR_{TH} is applied. As mentioned above, the threshold condition is related to noticeability not acceptability. Thus, the proposed method could be applied more flexibly as one's preference.

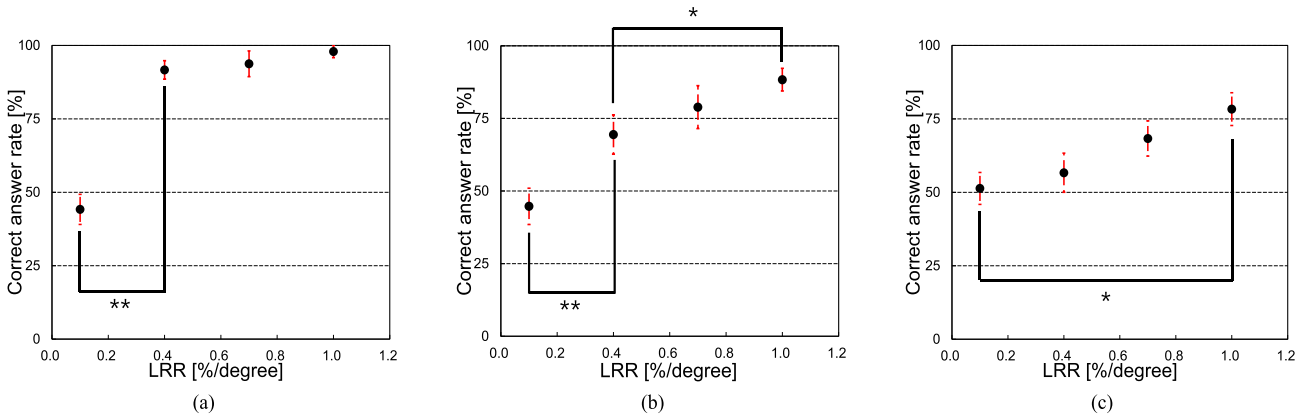

FIGURE 8. Average correct answer rate per LRR condition and statistical analysis of (a) Seaside, (b) Deer, and (c) Field clips. *$p < 0.05$, **$p < 0.01$.

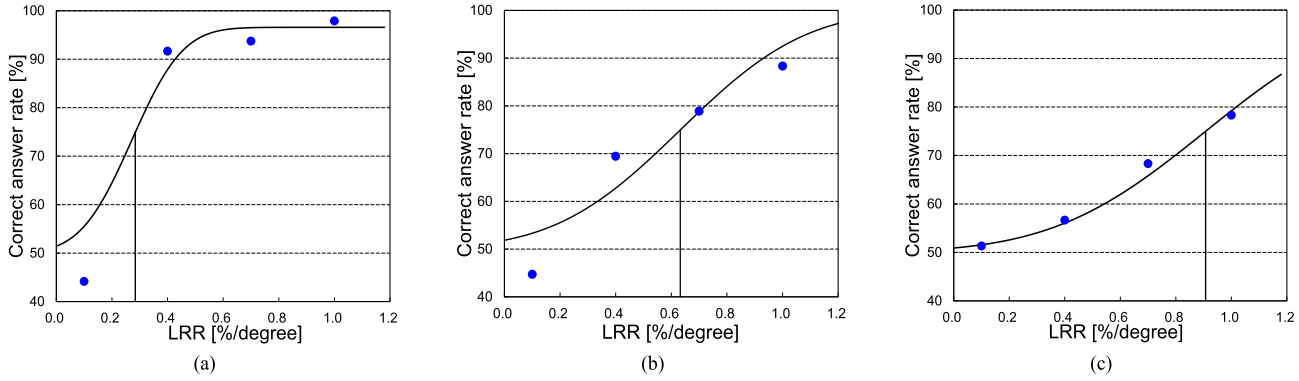

FIGURE 9. Psychometric function and threshold levels of (a) Seaside, (b) Deer, and (c) Field clips.

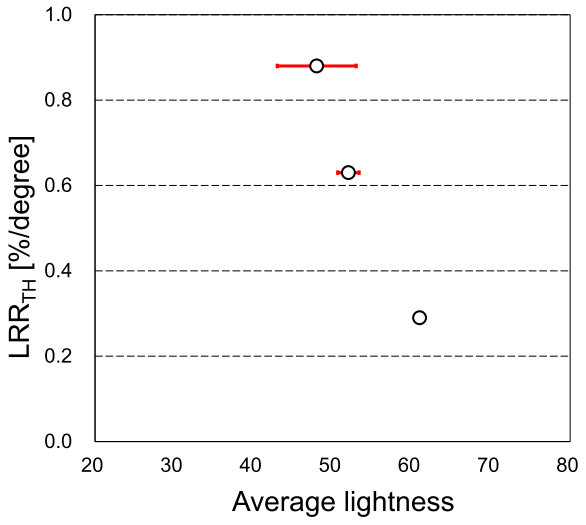

FIGURE 10. LRRTH depending on the average lightness of the clip.

TABLE 4. Amount of the total dissipated power and saved power.

	Seaside	Deer	Field
TDP_{ORG}	5.1×10^{13}	2.9×10^{13}	2.7×10^{13}
TDP_{TH}	4.5×10^{13}	2.3×10^{13}	1.7×10^{13}
Mean P_{SAVED} [%]	11.0	21.0	34.4

B. COMPARISON WITH PREVIOUS STUDIES

In this section, we compare the proposed method with previous studies, PCCE [11] and two BS [8], [13] methods. The PCCE is one of the most widespread CE techniques, and the two BS techniques presented in [8] and [13] reduce the brightness by modulating the Y (YCbCr) and L* (CIELAB) components, respectively. Because the three methods commonly have a similar approach that reduces the brightness, we chose them for comparison.

In our study, the subjective IQA was performed to obtain the results. However, LRR_{TH}s are not suitable for comparing the performance because most of them are based on the objective IQA. Thus, we calculate the structural similarity (SSIM) index [29] which is the most widely used objective image quality metric. The SSIM index is calculated on a 2D map, and the value of the global mean SSIM (MSSIM) was used. The MSSIM value is obtained in the range of 0–1, where 1 indicates that two images are identical. We computed the MSSIM for the overall frame images and then averaged them. The MSSIM values were obtained under the same P_{SAVED} condition, as described in Table 5. The MSSIM values are in the range of 0.9481–0.9943 when our method is applied. Other methods also have high MSSIM values of over 0.9, except for 0.8384. The results of the proposed method are higher than those of the CE method and lower than those of

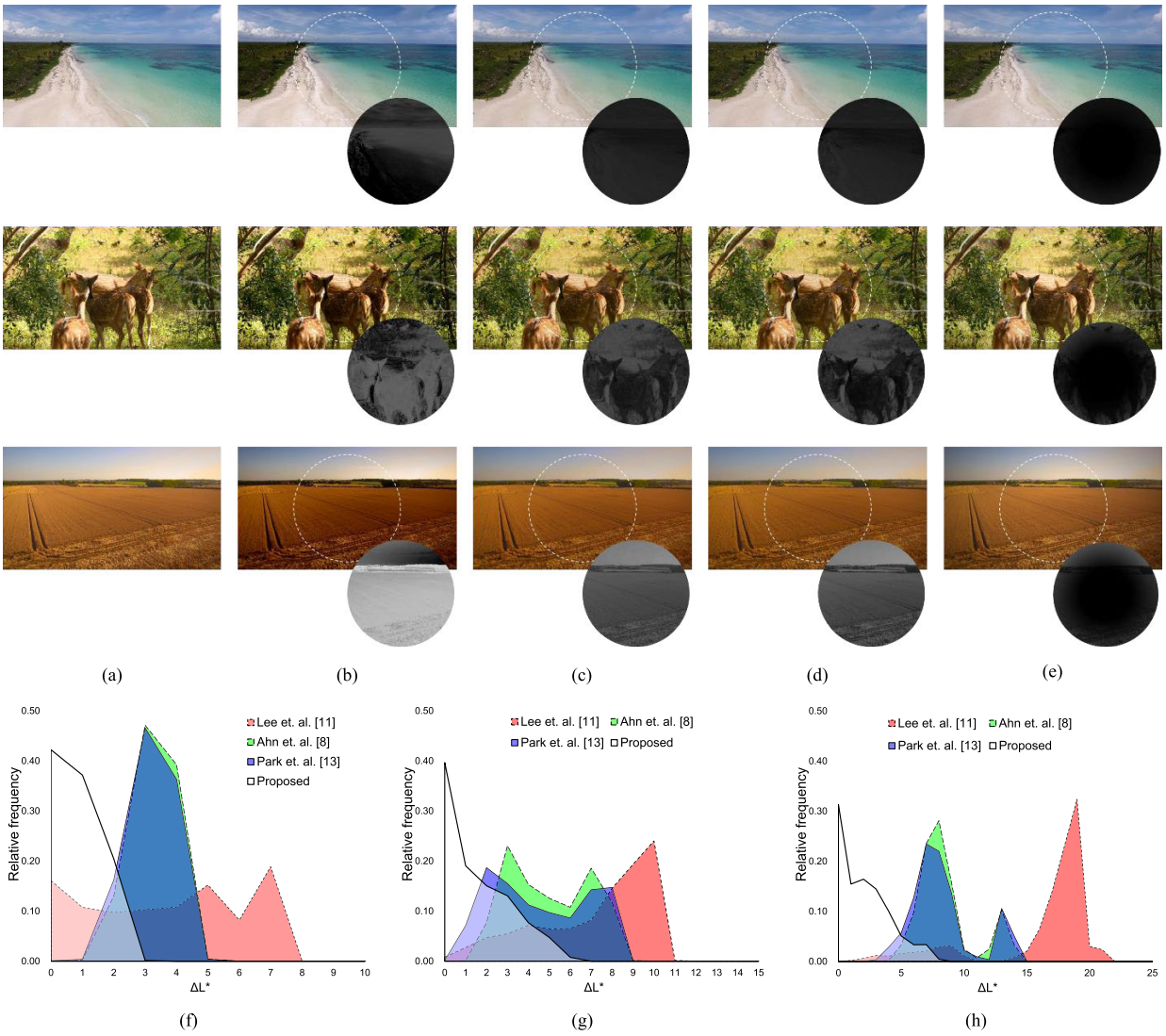

FIGURE 11. Visual comparison between (a) the original images and the modified images generated by (b) [11], (c) [8], (d) [13], and (e) the proposed method. The circular images illustrate ΔL^* within the area between the original and modified images. Distribution graphs of ΔL^* of (f) Seaside, (g) Deer, and (h) Field images.

TABLE 5. Objective image quality Comparison of the proposed method with previous studies.

Video	MSSIM				P_{SAVED} [%]
	Lee *et al.* [11]	Ahn *et al.* [8]	Park *et al.* [13]	Proposed method	
Seaside	0.9820	0.9971	0.9980	0.9943	11.0
Deer	0.9239	0.9887	0.9911	0.9717	21.0
Field	0.8384	0.9656	0.9751	0.9481	34.4

the two BS methods. However, all results are high scores, which indicates that the image quality degradation is negligible. From these results, it is verified that the proposed method could maintain the objective image quality as well.

Fig. 11 shows a visual comparison of the images generated by the proposed and previous methods. As shown in Fig. 11 (b), the CE method improves the contrast but makes the images noticeably darker. Unlike the CE method, it is difficult to notice any difference between the original and generated images, as shown in Fig. 11(c)–11(e). Note that the goal of the proposed method is not to improve the image quality but to maintain the perceived image quality. Thus, we focused on observing changes in the image quality in the visual field. The white dashed circles indicate a field of view of 20°. The circular monochromic images illustrate the lightness difference (ΔL^*) within the area between the original and modified images. The circular images were obtained by multiplying ΔL^* by 10 to highlight the visual difference.

Thus, the brighter the circular image is, the larger the visual difference is. As shown in Fig. 11(b)–11(e), the circular images of the previous methods are considerably brighter than ours, which indicates that our method maintains the image brightness in the visual field. Fig. 11(f)–11(h) show the distribution of ΔL^*. The white, red, green, and blue colored distributions indicate the proposed and previous methods of [11], [8], and [13], respectively. On one hand, in the case of the proposed method, it is observed that a majority of the ΔL^* values are zero and are distributed near zero. On the other hand, the ΔL^* distributions of the previous methods (in red, green, and blue) are skewed to the right. This indicates that the proposed method has the least decrease in the image brightness in the visual field, which is the most important part of human vision. It is widely known that brightness is correlated to image contrast, which is an important factor in perceived image quality. The CE technique enhances the image contrast but greatly reduces the global brightness, as compared with other techniques. In the case of the two BS techniques, their reduced brightness would lead to lower image contrast. Consequently, we believe that the proposed method is the most advantageous low-power technique in terms of maintaining the original image quality.

These results show that the proposed method does not worsen the image quality significantly, either objective or subjective, in terms of visual perception. Furthermore, our method employs interaction with the eye tracker; hence, the perceived image quality can be maintained even when the users move their gaze.

VI. CONCLUSION

In this paper, we propose a new low-power technology, called peripheral dimming, for OLED displays. Peripheral dimming saves power consumption by reducing the luminance of the area that corresponds to the peripheral vision area. A psychophysical experiment with a gaze point at the screen center was conducted. The LRR_{TH} conditions of three different video clips were obtained, and it was observed that LRR_{TH} is inversely proportional to the average lightness of the video. We anticipate that a quantitative model of LRR_{TH} depending on the image will be clearly determined in further studies. The proposed method can save the power up to 34.4% while maintaining the perceptual image quality and the objective quality (less than 6% drop in the MSSIM).

The goal of our study is to establish conditions for universal application of the proposed technique. The proposed method is a low-power technique, which is adequate for self-luminous displays such as OLED and micro-LED displays used for HMDs. Recently, stand-alone HMD devices with an integrated eye tracker have been released. If this trend continues, the critical problem of the need for an eye tracker for applying the proposed method is solved. Moreover, as stand-alone HMD devices would be battery-powered, a low-power technique is essential for them. Therefore, we believe that the peripheral dimming method will become an attractive technique in VR and AR devices.

REFERENCES

[1] A. Nathan, G. R. Chaji, and S. J. Ashtiani, "Driving schemes for a-Si and LTPS AMOLED displays," *J. Display Technol.*, vol. 1, no. 2, pp. 267–277, Dec. 2005.

[2] C.-L. Lin, K.-W. Chou, C.-C. Hung, and C.-D. Tu, "Lifetime amelioration for an AMOLED pixel circuit by using a novel AC driving scheme," *IEEE Trans. Electron Devices*, vol. 58, no. 8, pp. 2652–2659, Aug. 2011.

[3] C.-L. Lin and T.-T. Tsai, "A novel voltage driving method using 3-TFT pixel circuit for AMOLED," *IEEE Electron Device Lett.*, vol. 28, no. 6, pp. 489–491, Jun. 2007.

[4] M. Ohta, H. Tsutsu, H. Takahara, I. Kobayashi, T. Uemura, and Y. Takubo, "A novel current programmed pixel for active matrix OLED displays," in *SID Int. Symp. Dig. Tech. Papers*, May 2003, vol. 34, no. 1, pp. 108–111.

[5] D. Shin, Y. Kim, N. Chang, and M. Pedram, "Dynamic driver supply voltage scaling for organic light emitting diode displays," *IEEE Trans. Comput.-Aided Design Integr. Circuits Syst.*, vol. 32, no. 7, pp. 1017–1029, Jul. 2013.

[6] H. Oh, J.-H. Yang, G. H. Kim, H. Lee, B.-H. Kwon, C. Byun, C.-S. Hwang, K. I. Cho, and J.-I. Lee, "Light- and space-adaptable display," *J. Inf. Display*, vol. 19, no. 4, pp. 165–170, Oct. 2018.

[7] A. Arkhipov, B. W. Lee, K. T. Park, S. D. Sung, T. S. Shin, and K. H. Chung, "Using net power control for AMOLED TV," in *IMID Dig.*, Aug. 2007, vol. 7, no. 1, pp. 47–50.

[8] Y. Ahn and S. J. Kang, "OLED power reduction algorithm using gray-level mapping conversion," in *SID Int. Symp. Dig. Tech. Papers*, Jun. 2015, vol. 46, no. 1, pp. 254–257.

[9] X. Chen, Y. Chen, and C. J. Xue, "DaTuM: Dynamic tone mapping technique for OLED display power saving based on video classification," in *Proc. 52nd Design Automat. Conf.*, Jun. 2015, pp. 1–6.

[10] D. J. Pagliari, S. Di Cataldo, E. Patti, A. Macii, E. Macii, and M. Poncino, "Low-overhead adaptive brightness scaling for energy reduction in OLED displays," *IEEE Trans. Emerg. Topics Comput.*, early access, Mar. 29, 2019, doi: 10.1109/TETC.2019.2908257.

[11] C. Lee, C. Lee, Y.-Y. Lee, and C.-S. Kim, "Power-constrained contrast enhancement for emissive displays based on histogram equalization," *IEEE Trans. Image Process.*, vol. 21, no. 1, pp. 80–93, Jan. 2012.

[12] D. J. Pagliari, E. Macii, and M. Poncino, "LAPSE: Low-overhead adaptive power saving and contrast enhancement for OLEDs," *IEEE Trans. Image Process.*, vol. 27, no. 9, pp. 4623–4637, Sep. 2018.

[13] M. Park and M. Song, "Saving power in video playback on OLED displays by acceptable changes to perceived brightness," *J. Display Technol.*, vol. 12, no. 5, pp. 483–490, May 2016.

[14] P. K. Choubey, A. K. Singh, R. B. Bankapur, P. C. S. B. Vaisakh, and M. B. Prabhu, "Content aware targeted image manipulation to reduce power consumption in OLED panels," in *Proc. 8th Int. Conf. Contemp. Comput. (IC)*, Aug. 2015, pp. 467–471.

[15] B. Anand, L. Kecen, and A. L. Ananda, "PARVAI-HVS aware adaptive display power management for mobile games," in *Proc. 7th Int. Conf. Mobile Comput. Ubiquitous Netw.*, Jan. 2014, pp. 21–26.

[16] T. K. Wee and R. K. Balan, "Adaptive display power management for OLED displays," in *Proc. 1st ACM Int. Workshop Mobile Gaming*, Aug. 2012, pp. 25–30.

[17] X. Chen, K. W. Nixon, H. Zhou, Y. Liu, and Y. Chen, "FingerShadow: An OLED power optimization based on smartphone touch interactions," in *Proc. 6th Workshop Power-Aware Comput. Syst.*, Berkeley, CA, USA, 2014, pp. 1–5.

[18] A. Patney, J. Kim, M. Salvi, A. Kaplanyan, C. Wyman, N. Benty, A. Lefohn, and D. Luebke, "Perceptually-based foveated virtual reality," in *Proc. ACM SIGGRAPH Emerg. Technol.*, Jul. 2016, pp. 1–2.

[19] M. Dong and L. Zhong, "Power modeling and optimization for OLED displays," *IEEE Trans. Mobile Comput.*, vol. 11, no. 9, pp. 1587–1599, Sep. 2012.

[20] M. Dong, Y.-S.-K. Choi, and L. Zhong, "Power modeling of graphical user interfaces on OLED displays," in *Proc. 46th Annu. Design Automat. Conf. (ZZZ-DAC)*, San Francisco, CA, USA, Jul. 2009, pp. 652–657.

[21] D. J. Pagliari, E. Macii, and M. Poncino, "Optimal content-dependent dynamic brightness scaling for OLED displays," in *Proc. 27th Int. Symp. Power Timing Modeling, Optim. Simulation (PATMOS)*, Thessaloniki, Greece, Sep. 2017, pp. 1–6.

[22] G. Osterberg, "Topography of the layer of rods and cones in the human retina," in *Acta Ophthalmologica Supplement*. Copenhagen, Denmark: Levin Munksgaard, 1935, pp. 1–102.

[23] E. F. Schubert, "Human eye sensitivity and photometric quantities," in *Light-Emitting Diodes*, 2nd ed. Cambridge, U.K.: Cambridge Univ. Press, 2006, pp. 275–291.
[24] G. A. Gescheider, "Psychophysical measurement of thresholds: Differential sensitivity," in *Psychophysics: The Fundamentals*, 3rd ed. New York, NY, USA: Psychology Press, 2013, pp. 1–15.
[25] H. H. Schütt, S. Harmeling, J. H. Macke, and F. A. Wichmann, "Painfree and accurate Bayesian estimation of psychometric functions for (potentially) overdispersed data," *Vis. Res.*, vol. 122, pp. 105–123, May 2016.
[26] *Methodology for the Subjective Assessment of the Quality of Television Pictures*, document ITU-R Rec. BT.500-11, 2002.
[27] M. Jogan and A. A. Stocker, "A new two-alternative forced choice method for the unbiased characterization of perceptual bias and discriminability," *J. Vis.*, vol. 14, no. 3, pp. 20–38, Mar. 2014.
[28] Pixabay, München, Germany. *Sea-Deer-Cornfield*. Accessed: Oct. 11, 2017. [Online]. Available: https://pixabay.com/
[29] Z. Wang, A. C. Bovik, H. R. Sheikh, and E. P. Simoncelli, "Image quality assessment: From error visibility to structural similarity," *IEEE Trans. Image Process.*, vol. 13, no. 4, pp. 600–612, Apr. 2004.

JEONG-SIK KIM received the B.S. and M.S. degrees in information display from Kyung Hee University, Seoul, South Korea, in 2016 and 2018, respectively, where he is currently pursuing the Ph.D. degree with the Department of Information Display. He has been involved in driving technology for visibility, color, and motion performance of the displays.

SEUNG-WOO LEE (Senior Member, IEEE) received the B.S. and M.S. degrees in electrical engineering and the Ph.D. degree from the Korea Advanced Institute of Science and Technology in 1993, 1995, and 2000, respectively, where he conducted research on integrated driver circuits for poly-Si TFT-LCDs. He joined Samsung, in 2000, where his work has focused on the development of key driving technologies for active-matrix liquid-crystal displays. He has played a key role in image quality enhancement, high-end LCD timing-controller design, FPGA evaluation of new driving schemes, next-generation LCD interface technologies, and advanced LCD driving schemes for large-size TV applications. He was also in charge of the development of analog–digital mixed-signal ICs for TFT-LCDs. He joined Kyung Hee University, Seoul, South Korea, where he has been studying novel display systems and visual perception. He is currently a Full Professor with the Department of Information Display. He was a recipient of the 2008 Chester Sall Award from the IEEE Consumer Electronics Society in 2010. He has been active as a Senior Member of the Society for Information Display since 2010.